

FEEDBACK CONTROL OF A CIRCULAR CYLINDER WAKE IN A WATER TUNNEL EXPERIMENT

Stefan Siegel*, Kelly Cohen**, Tom McLaughlin†

*Department of Aeronautics
U.S. Air Force Academy, Colorado Springs, CO 80840, USA*

Abstract

The effect of feedback flow control on the wake of a circular cylinder at a Reynolds numbers of 100 is investigated in a water tunnel experiment. Our control approach uses a low dimensional model based on proper orthogonal decomposition (POD). The controller applies linear proportional and differential feedback to the estimate of the first POD mode. A 7 Sensor configuration implemented in Real Time PIV is used to measure flow velocity. Mode amplitudes are estimated in real time using Linear Stochastic Estimation (LSE). The accuracy of the LSE estimate of the mode amplitudes is explored in detail. In the context of this application, actuation is implemented as displacement of the cylinder normal to the flow. Using transient open loop forcing we demonstrate that there is a threshold peak amplitude below which the control actuation ceases to be effective. This threshold is identical to the threshold as determined by 2D CFD simulations.

The closed loop feedback experiments are conducted to confirm findings of two-dimensional CFD simulations which showed the ability of feedback flow control to reduce both unsteady lift and drag. While neither of these quantities is easily measured in our experiment, we compare the global effect of feedback control in both CFD simulation and PIV measurements in the water tunnel on the flow field and find good agreement.

The closed loop experiments using a fixed gain strategy show good agreement to CFD simulations. While the amplitudes of the POD modes can be temporarily reduced with appropriate controller gains, both experiment and simulation are not able to stabilize the flow field in this state for extended periods of time.

Introduction

Two-dimensional bluff body wakes have been investigated for quite some time. In a two-dimensional cylinder wake, self-excited oscillations in the form of periodic shedding of vortices are observed above a critical Reynolds number of approximately 47. This behavior is referred to as the von Kármán Vortex Street. According to Williamson¹, the regime of laminar vortex shedding extends to a Reynolds number of approximately 180, before three-dimensional instabilities occur. This is the Reynolds number regime that we target in this investigation. However, the Kármán vortex street as the fundamental feature of this type of wake flow is sustained to very large Reynolds numbers (on the order of millions).

Therefore many lessons learned at low Reynolds numbers will still be applicable to applications of practical interest at much higher Reynolds numbers.

The nonlinear oscillations of the vortex street lead to some undesirable effects associated with unsteady pressures such as fluid-structure interactions² and lift/drag fluctuations³. Also, the vortices themselves greatly increase the drag of the bluff body, compared to the steady wake that can be observed at lower Reynolds numbers. Monkewitz⁴ showed that the von Kármán Vortex Street is the result of an absolute, global instability in the near wake of the cylinder. Further downstream the flow is convectively unstable. This absolute instability is causing the flow to behave as a self sustained oscillator, with internal positive feedback leading to temporal amplification of the oscillation by the recirculation region downstream of the cylinder.

Many attempts to improve the unsteady vortex street have been made. When active open loop forcing of the wake is employed, the vortex shedding in the wake can be locked in phase to the forcing signal⁵. While these find-

* Assistant Research Associate, Member

** Visiting Researcher, Member

† Research Associate, Associate Fellow

This paper is declared a work of the U.S. Government and is not subject to copyright protection in the United States

ings suggest that the dominant structures in the flow field can be influenced by the forcing, it also strengthens the vortices, and, consequently increases the mean drag as well as unsteady lift fluctuations. Different forcing methods are effective in influencing the behavior of the flow. Acoustic excitation of the wake, longitudinal, lateral or rotational vibration of the cylinder model, and alternate blowing and suction at the separation points⁵ have been used. Using these methods, the flow exhibits regions of lock-in and non-lock-in. Lock-in is defined as the flow exhibiting a fixed phase relationship to the forcing. Koopmann⁶ experimentally investigated these regions, and found that the lock-in frequency range de-

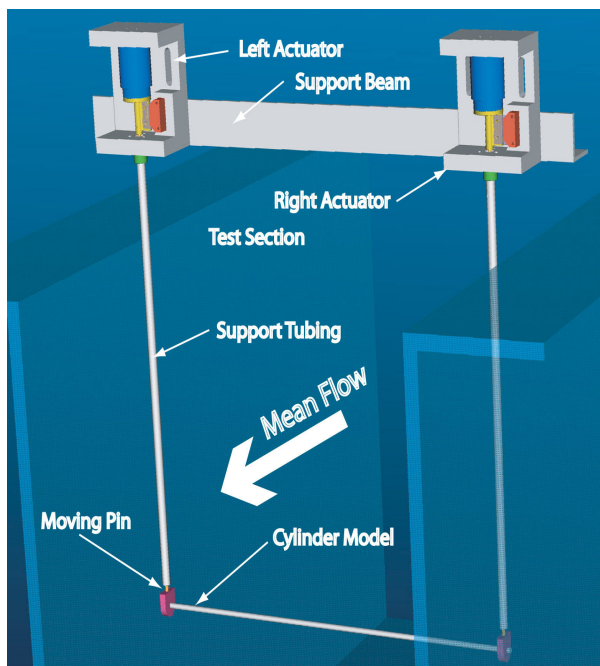


FIGURE 1 Water Tunnel Experiment Setup

pendes on the forcing amplitude. The higher the forcing amplitude, the larger the frequency band for which he could achieve lock-in. Additionally, even at the natural vortex shedding frequency, he found a minimum threshold amplitude that was needed for lock-in to occur. For the cylinder wake, all of these open loop forcing methods have not been shown to reduce the drag, independent of frequency and amplitude employed. The only exceptions are situations where the separation point location is shifted. It should be noted that the geometry of a circular cylinder lends itself to active control methods that target the separation point location of the flow rather than the absolute instability of the wake itself. Using methods like periodic blowing and suction on the cylinder surface in a fashion similar to that employed on the

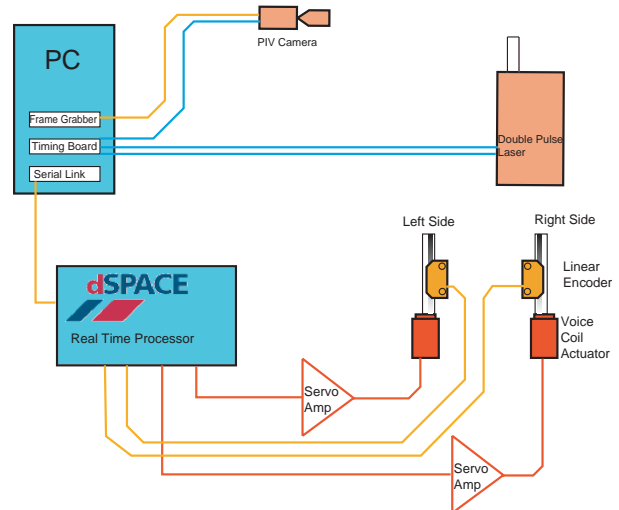


FIGURE 2 Hardware Setup

suction side of airfoils, the separation point can be moved aft which in turn will lead to a narrower wake. A narrower wake will exhibit improved instability characteristics, in addition to lower drag due to a lower velocity deficit in and by itself. This effect can be observed in the natural cylinder wake during the “drag crisis”, when boundary layer transition occurs upstream of the separation point, and the resulting turbulent boundary layer shifts the separation point downstream. Thus feedback control investigations using periodic blowing and suction like those employed by Min and Choi⁷ actually employ two flow control techniques simultaneously, namely separation control and wake stabilization due to feedback. It is difficult if not impossible to judge what portion of the improvement is due to either of these techniques in their simulations.

The only way of suppressing the self-excited flow oscillations without altering the mean flow is by the incorporation of active closed-loop flow control⁸. Traditionally, several fundamentally different approaches to achieve feedback flow control have been employed. The mathematically driven approach to develop a control scheme is hampered by the complexity of the governing Navier Stokes equations. In order to tackle this complexity, one needs to make simplifying assumptions. At this point, the assumptions made in simplifying the equations have often rendered the results inapplicable to real life experiments(Li and Aubry⁹). It is imperative to ensure that assumptions made in the controller derivation do not render the controller incapable of dealing with the physics of the flow field. An alternative approach uses optimal control theory, and the resulting control algorithm (if it can be derived at all with today’s com-

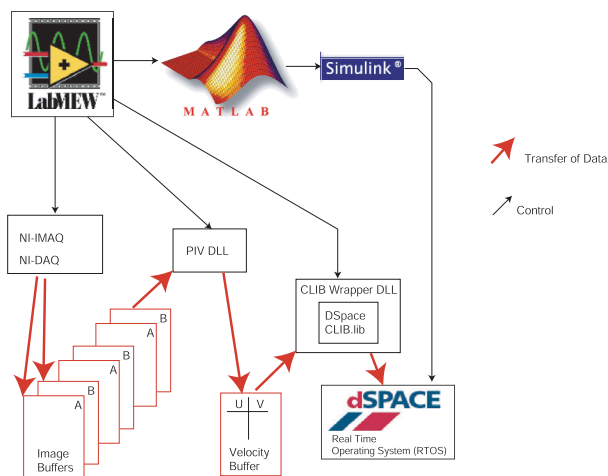


FIGURE 3 Software Setup

puting capabilities) is often too complex to be implemented in real time (Bewley and Trenchea¹⁰).

On the other hand, approaching the controls problem using an experimental / empirical approach with no modeling of the physics of the flow yields poor results also. Experimental studies conducted by Roussopoulos² show that a linear proportional feedback control based on a single sensor feedback is able to delay the onset of the wake instability only slightly, rendering the wake stable at Re about 20% higher than the unforced case. Roussopoulos reports that above Re = 60, a single-sensor feedback may suppress the original mode but destabilizes one of the other modes. Therefore, bet-

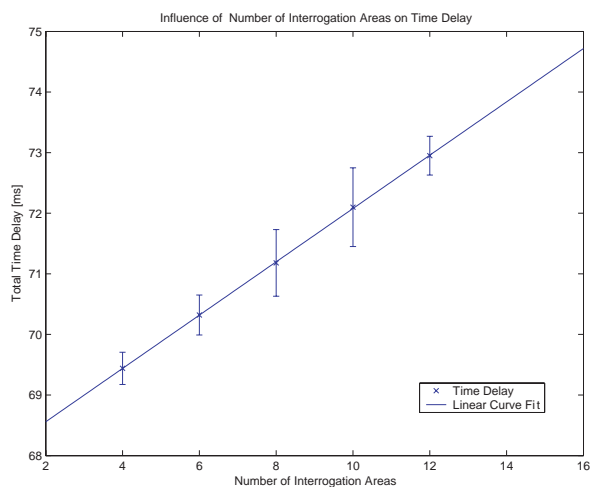


FIGURE 4 Time Delay for different numbers of interrogation areas. Interrogation area extracted from first image is 32 x 32 pixels in size, interrogation area from second image is 40 x 40 pixels. Total time delay averaged over 32 acquisitions, error bars depict one standard deviation.

ter control strategies are needed to stabilize the wake at Reynolds numbers of technical interest.

An alternate approach to this problem lies in the development of a low order model of the flow. The model can be used both for controller development, as well as flow field state estimation. Ideally, it reduces the complexity of the governing Navier Stokes equations to

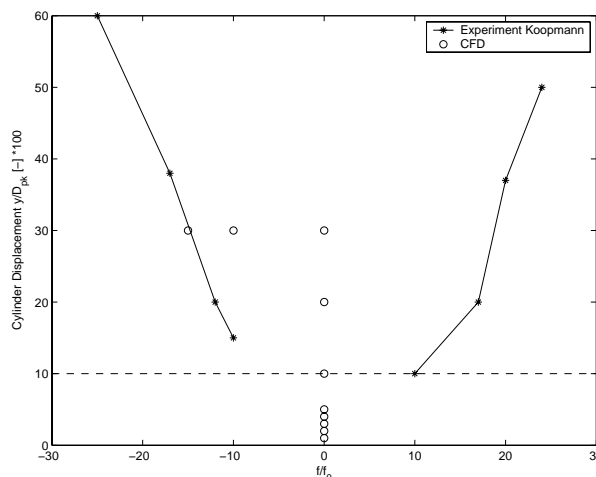


FIGURE 5 Lock-in region adapted from Koopman(1966) CFD data points are from Siegel et al.²³. We will show water tunnel data in the final version of this graph.

a level that the model can be implemented in real time, while still capturing the important physics of the flow. Gillies¹¹ pioneered the application of this technique to cylinder wakes by developing a low dimensional model of the cylinder wake at a Reynolds number of 100. Cohen et al.¹² have shown that using this model, the cylinder wake model flow can be successfully controlled using a relatively simple linear control approach based on the most dominant mode only. Siegel et al.²³ proceeded to apply this control approach successfully to a full, two-dimensional Navier Stokes simulation of the flow field. While they were able to stabilize the near wake, the far wake was beyond the reach of the actuation provided by the cylinder displacement normal to the flow. Nonetheless, they were able to reduce the unsteady lift force by more than 90%, and achieved an overall reduction in drag of 15%.

The goal of this paper is to apply the feedback control approach used by Siegel et al.²³ to a water tunnel experiment. A limited number of sensors are used to estimate the state of the low dimensional model that characterizes the flow. The controller then acts on the flow state estimates in order to determine the actuator displacement (Figure 1 shows the overall setup of this experiment).

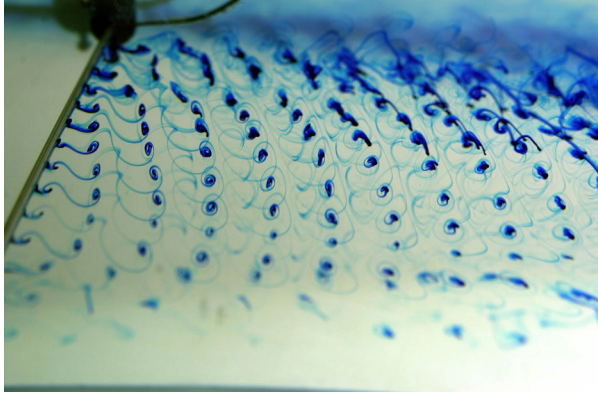


FIGURE 6 Flow Visualization of the wake at $Re = 120$, unforced

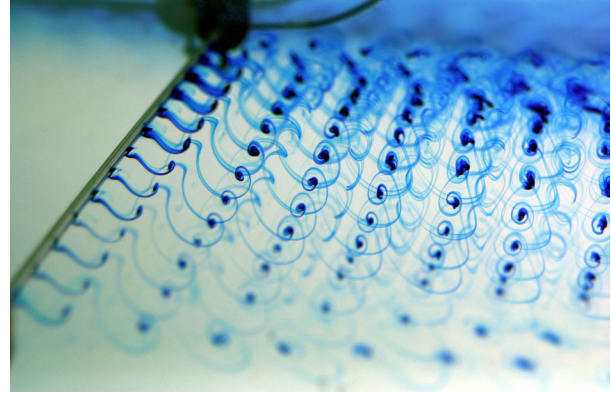


FIGURE 7 Flow Visualization of the cylinder wake at $Re = 120$, forced at the natural shedding frequency with an amplitude of 30% of the cylinder diameter

Experimental Setup

Feedback flow control experimentation poses severe demands on measurement, actuation and real time processing equipment. In order to implement this experiment, we found a water tunnel environment most favorable. It provides good flow quality at low speeds, while allowing for relatively large model size and thus for a low shedding frequency. This reduces demands on the bandwidth of actuators, sensors and real time processing computer hardware.

Water Tunnel Facility

All experiments were conducted in the USAF Academy 38 cm x 110cm free-surface water tunnel. This is a commercially available unit manufactured by Eidetics, Model 1520.

Model and Forcing Setup

A precision ground stainless steel rod of 6.35 mm diameter served as the cylinder model. It was suspended in the center of water tunnel by two translating pins flush with the tunnel wall, as shown in Figure 1. The position of the translating pins was controlled by two independent voice coil actuators, which in connection with a precision linear quadrature encoder and Proportional and Differential (PD) controller provided positioning capability with a resolution of $0.4\mu\text{m}$. The cylinder model is fitted with end disk slanted at 10 degrees (Williamson¹) and has an aspect ratio of more than 80. At a Reynolds number of 100 and typical water temperatures, this cylinder model will develop a natural shedding frequency in the order of 0.4 Hz.

Real Time Particle Image Velocimetry (RTPIV)

The authors of this study developed a real time capable digital Particle Image Velocimeter (RTPIV) whose details are described in a previous publication²². This system enables multiple non-intrusive velocity sensor locations in the wake with an update rate of up to 15 Hz. An overview of the hardware configuration is shown in Figure 2, the software implementation is shown in Figure 3. Results of a time delay study of the PIV setup are reproduced in Figure 4. With a typical time delay in the order of 70 ms corresponding to less than ten percent of a shedding cycle, no severe robustness requirements are imposed on the controller. The particle displacement for all PIV measurements was adjusted such that the overall velocity measurement uncertainty was less than 5 % of the freestream velocity. The interrogation area size was kept at less than 10% of the cylinder diameter, thus setting the spatial resolution at that value.

Flow Visualization

While the RTPIV system allows for quantitative velocity measurements in a single measurement plane, flow visualization is the experimental technique of choice to check the flow field for spanwise coherence. Since our current control approaches assume a two-dimensional flow field, it is imperative to verify the two-dimensionality in the experiment. While flow visualization is typically only a qualitative technique, it can be used successfully to check the flow for two-dimensionality. Figure 6 shows the flow field without forcing, Figure 7 with forcing. It can be seen that the forcing establishes spanwise coherence, and thus two-dimensionality in the flow, which is otherwise absent.

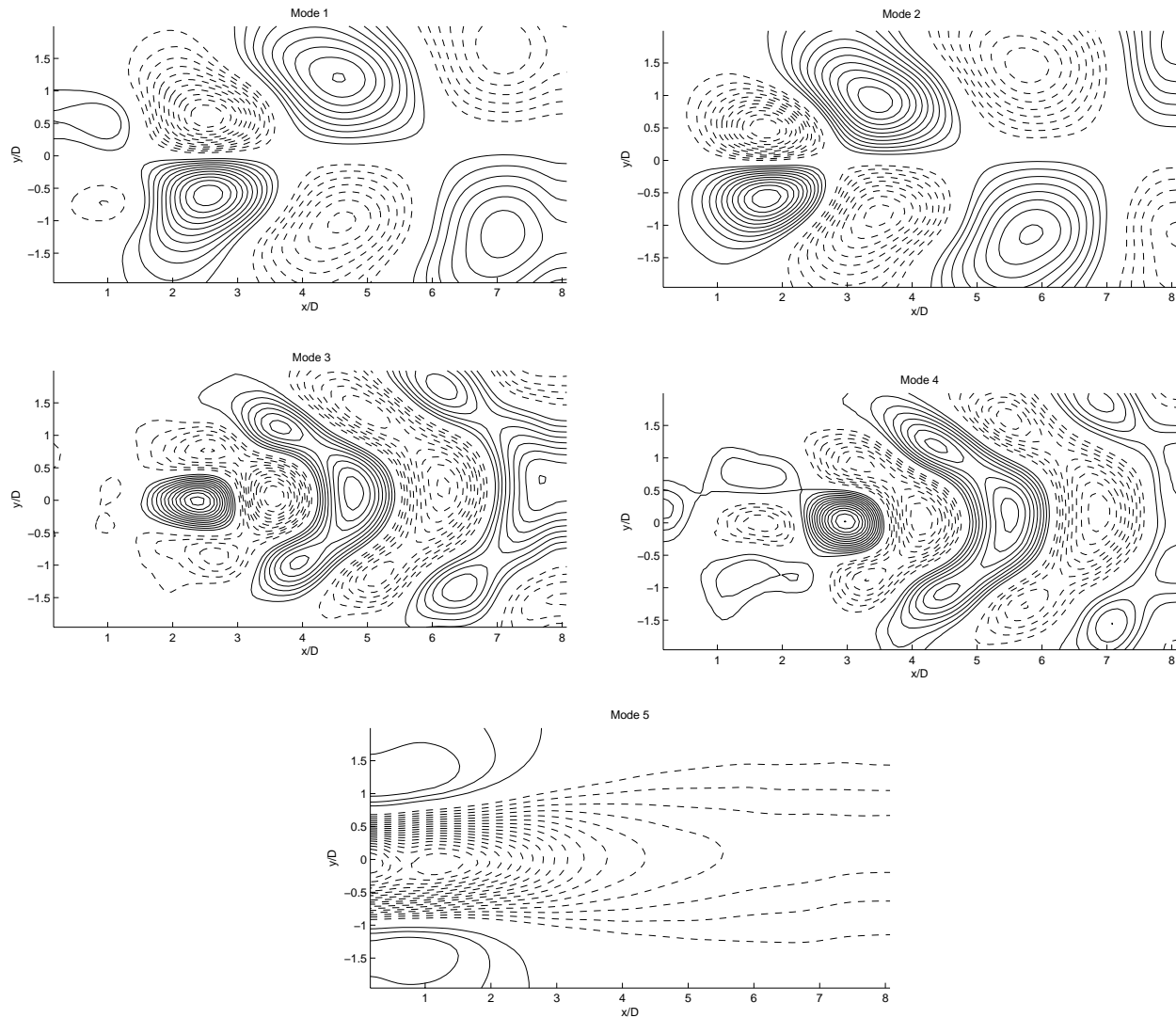


FIGURE 8. Eigenfunctions of the 5 Mode POD model based on water tunnel data at $Re = 120$, using the U velocity component as input for the POD decomposition. Solid lines are positive, dashed lines negative isocontours.

POD Modeling and Estimation

Feasible real time estimation and control of the cylinder wake may be effectively realized by reducing the model complexity of the cylinder wake as described by the Navier-Stokes equations, using POD techniques. POD, a nonlinear model reduction approach, is also referred to in the literature as the Karhunen-Loeve expansion¹⁵. POD decomposes a unsteady flow field into spatial modes and temporal mode amplitudes. The desired POD model contains an adequate number of modes to enable modeling of the temporal and spatial characteristics of the large-scale coherent structures inherent in the flow.

In this effort, the method of “snapshots” introduced by Sirovich¹⁶ is employed to generate the basis functions of the POD spatial modes from the PIV measurements.

Only the U velocity component (in the direction of the mean flow) was used for POD decomposition in this effort. This decision was made in order to be able to estimate the mode amplitudes based on sensor information, which in our experiment will yield the U and V component of velocity. Since the change in mean flow distribution is an important quantity, and the rms fluctuations in the U velocity are of higher amplitude, we chose the U velocity component over the V velocity component.

An important aspect of reduced order modeling concerns truncation: how many modes are important and what are the criteria for effective truncation? The answers to the above questions have been addressed by Cohen et al.¹² This effort showed that control of the POD model,

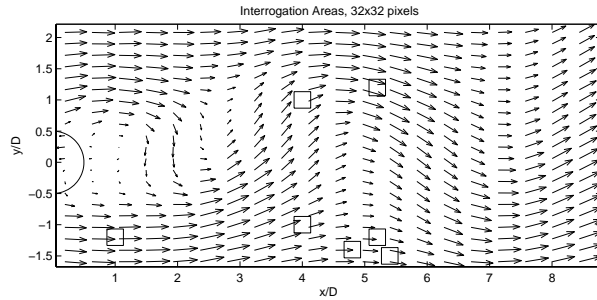


FIGURE 9 PIV Interrogation Areas of 7 Sensor Configuration superimposed on PIV velocity field downsampled by a factor of 2 in y and 5 in x direction.

of the von Kármán vortex street in the wake of a circular cylinder at $Re = 100$, is enabled using just the first mode. Furthermore, feedback based on the first mode alone suppressed all the other modes in a four mode POD model, indicating that higher order modes derive from the fundamental modes. In view of this result, truncation of the POD model took place after the first four

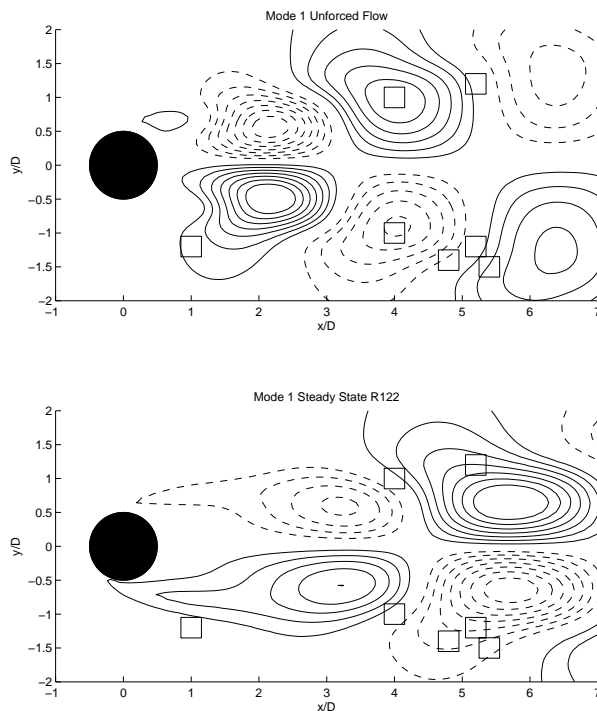


FIGURE 10 PIV Interrogation Areas of 7 Sensor Configuration superimposed on CFD derived POD Mode 1. Top, POD spatial modes from unforced flow data, bottom, POD spatial modes derived from feedback controlled steady state data.

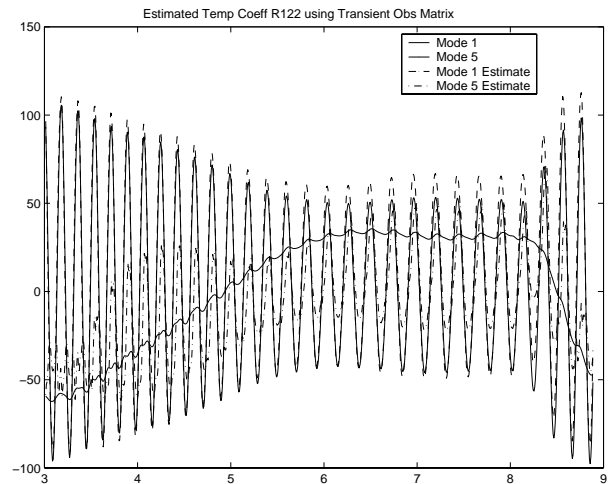
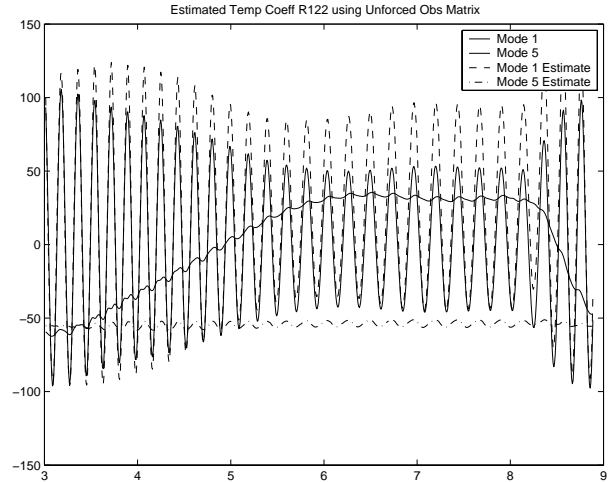


FIGURE 11 LSE Prediction of feedback controlled mode amplitudes based on 7 Sensor configuration. Top, LSE matrix developed from steady state unforced data. Bottom, LSE matrix developed from transient startup data.

modes, which contain more than 93.5% of the total amount of energy. At this point, it is imperative to note the difference between the number of modes required to reconstruct the flow and the number of modes required to control the flow. In this effort, we are interested in estimating only those modes required for closed-loop control. On the other hand, an accurate reconstruction of the velocity field based on a low-dimensional model may be obtained using between 4-8 modes.¹⁷ The POD algorithm was applied to the fluctuating velocity component in the direction of the flow as described in Equation (1). The decomposition of this component of the velocity field is as follows:

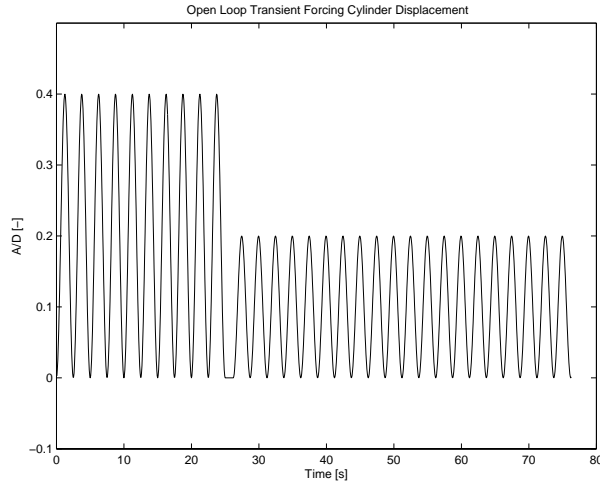


FIGURE 12 Transient forcing cylinder displacement for 10% A/D forcing amplitude

$$\tilde{u}(x, y, t) = U(x, y) + u(x, y, t) \quad (1)$$

where U [m/s] denotes the mean flow velocity and u [m/s] is the fluctuating component. It may be expanded as:

$$u(x, y, t) = \sum_{k=1}^n a_k(t) \phi_i^{(k)}(x, y) \quad (2)$$

where $a_k(t)$ denotes the time-dependent coefficients having units of m/s and $\phi(x, y)$ represent the non-dimensional spatial eigenfunctions (see Fig. 8) determined from the POD procedure. Shown are the first four modes of the POD decomposition, plus a 5th mode that was derived by subtracting the mean freestream velocity from the mean flow distribution of the unforced flow field. This mode was found to be necessary to obtain an estimate of the effect of feedback flow control onto the mean flow. It is being used to both estimate the effectiveness of the controller, as well as allow for gain scheduling to account for changes in the flow receptivity to forcing in a real time fashion. Additionally, Noack et al.¹⁸ have shown that adding a similar mode to account for changes in the mean flow greatly improves the ability of the model to account for transient effects in the flow field.

Once the spatial POD eigenfunctions have been derived, the corresponding time-dependent coefficients $a_k(t)$, or Mode amplitudes, need to be calculated. For this, two different schemes are reported in literature. Most often a Galerkin projection is used, which involves projecting the spatial eigenfunctions onto the Navier Stokes equations. This process involves spatial derivatives of the snapshots, which are, particularly in the case of experi-

mental data, inherently sensitive to noise. Gillies⁸ used a simple least squares fit, which we found to be much more robust.

Sensor Placement and Development of a Linear Stochastic Estimation Matrix

The experiment uses linear stochastic estimation (LSE) in order to estimate the mode amplitudes in real time. LSE is deterministic in terms of computing time, while least square fitting is not. Thus LSE is a much better choice for real time implementation. LSE uses an estimation matrix to derive the POD mode amplitudes based on sensor information. Cohen et al.²⁴ developed a heuristic approach to determine sensor locations based on the spatial POD mode distributions. Using this approach, two sensors were placed on the extrema of Mode 1, two more on the extrema of Mode 2, and one each on the extrema of Modes 3 and 4. A seventh sensor was placed in the free stream to aid detection of Mode 5. The resulting sensor setup is shown in Figure 9. Figure 10 shows the sensor locations superimposed on the spatial distribution of Mode 1. It is important to note that the spatial POD modes change as a result of feedback control, as is shown in Figure 10 by superimposing the same sensor locations onto the Mode 1 distribution derived from a stabilized feedback controlled CFD simulation. The POD mode has both shifted and stretched in the downstream direction and consequently the sensors are not perfectly aligned with the extrema of the spatial modes any more. This leads to an increase in estimation error as the controller becomes effective in stabilizing the wake.

Another issue in mode estimation is the data set used to derive the LSE estimation matrix. Figure 11 shows the ability of different LSE matrices to estimate the transient mode amplitudes of a feedback controlled simulation. For derivation of the matrix used for the top graph of Figure 11, steady state unforced data was used. This estimation matrix leads to large errors between the estimate and the actual mode amplitudes as soon as the controller becomes effective in reducing the mode amplitudes. The bottom graph shows estimates based on a matrix that was derived from transient startup data. This matrix enables reliable estimation of mode amplitudes throughout the entire feedback controlled run; with errors of less than 10% in amplitude for Mode 1 which is used for feedback. However, significant errors are present in particular for the estimate of the mean flow mode, Mode 5. Therefore this estimation matrix is useable for fixed gain feedback controlled experiments, which only rely on the feedback of Mode 1. It is not useable for variable gain feedback, which relies on an estimate of Mode 5 to update the controller gain.

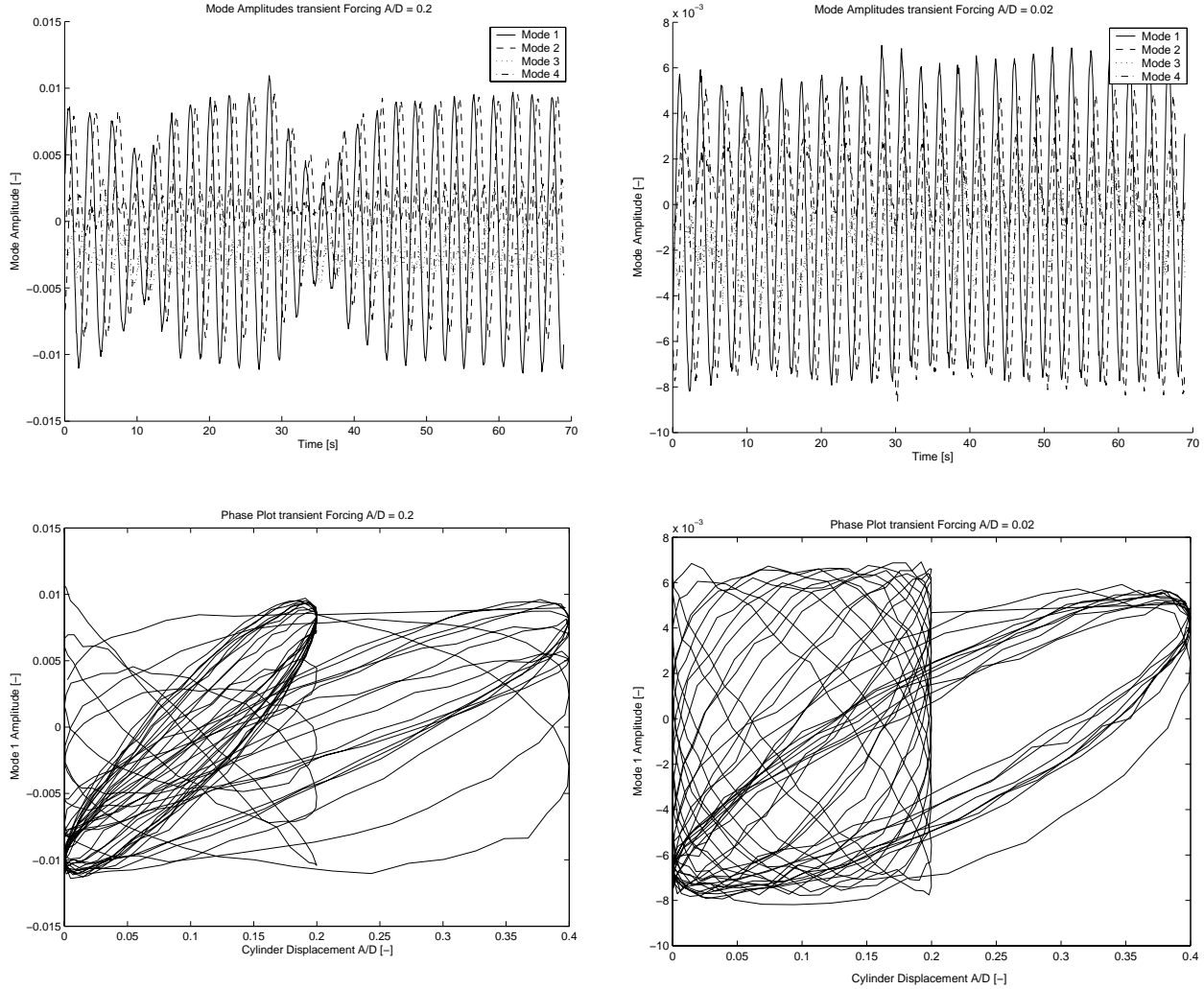


FIGURE 13 Transient forcing flow response for $A/D = 0.1$, left; and $A/D = 0.02$, right. Top, mode amplitudes, bottom, phase plots for mode 1.

The reliable estimation of transient flow fields is still ongoing research. We will present future improvements on low dimensional modeling and estimation, which are crucial to the success of feedback flow control.

For the feedback controlled runs, the sensor information at requested (x, y) locations in the flow is transferred to the DSpace system after correlating an image pair. The controller software then performs the linear stochastic estimation of the mode amplitudes.

Feedback Controller

The control algorithm acts on the estimate of the Mode 1 amplitude only. This design decision was made based on our earlier investigations controlling a low dimensional model of the flow. For the low dimensional model, proportional gain applied to Mode 1 only was sufficient

to suppress vortex shedding. We employed a Proportional and Differential (PD) feedback control strategy:

$$y_{cyl} = K_p \cdot a_1 + K_d \cdot \frac{da_1}{dt} \quad (3)$$

with y being the cylinder displacement. Instead of directly specifying the K_p and K_d gains, these can be expressed in terms of an overall gain K and a phase advance ϕ :

$$\begin{aligned} K_p &= K \cdot \cos(\phi) \\ K_d &= \frac{K \cdot \sin(\phi)}{2\pi f} \end{aligned} \quad (4)$$

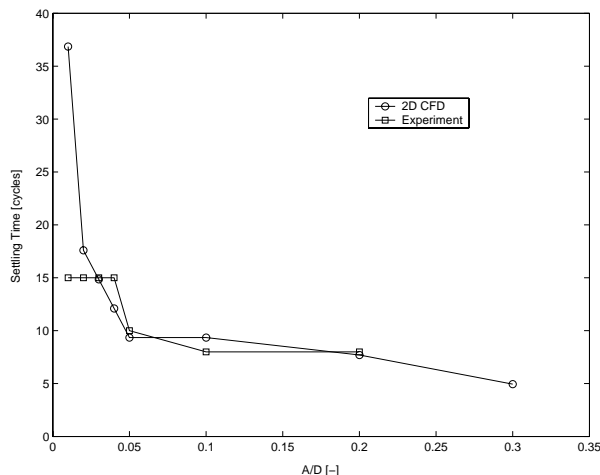


FIGURE 14 Comparison of settling times for CFD simulations and water tunnel experiments. The maximum detectable settling time in the experiments is 15 cycles.

With f being the vortex shedding frequency. Physically, the control algorithm was implemented in Simulink and compiled to run on a real time processor supplied by DSpace Inc., Model RT1103. This real time processor both implements the fluid dynamic feedback, as well as the PD controllers providing positioning of the cylinder model. Processing of the PIV data is interrupt driven and runs at a slower update rate (15Hz) than the PD controllers for positioning (10kHz). A hold filter is implemented in order to deal with failed correlations in individual interrogation areas, in case of a failed correlation the signal of the respective interrogation area is held at the previous value. A low pass filter is employed in order to reduce high frequency noise in the feedback path, its cutoff frequency is four times the natural shedding frequency.

Results

Transient Open Loop forcing

Before closing the loop, we investigated the lock-in range depending on forcing amplitude and frequency in detail. Lock-in has been essential in our CFD investigations, and we repeated the study in the experiment. Since the phase of the natural shedding is not known a priori, we first phase locked the vortex shedding by forcing the flow with a sinusoidal displacement that is known to result in lock-in. This was done for 10 shedding cycles forcing at the natural shedding frequency with a displacement of

20% of the cylinder diameter, as shown in Figure 12. After lock in has been achieved, the forcing was shifted by 180 degrees of phase and adjusted in amplitude to the value to be investigated. Figure 13 shows results for this type of forcing using an amplitude resulting in lock in (20%), on the left. Since the initial phase between natural shedding and forcing is random, a transient flow response can be observed within the first ten cycles. After the lock in has been achieved, a second transient which is the result of the phase shift in forcing can be observed. This is the transient of interest, and it lasts for about 8 shedding cycles for the case presented. After this a stable limit cycle is achieved again, as seen in the phase plot at the left bottom of figure 13. In a situation where no lock-in is achieved, (using a forcing amplitude of 2%), right portion of Figure 13, no stable limit cycle is achieved, which indicates the loss of controllability at this forcing amplitude.

Figure 14 summarizes the experimental findings for the settling time as a function of forcing amplitude, and compares them to the results of 2D CFD simulation runs as reported in Siegel et al²³. The observation time in the experiment is limited to 15 shedding cycles, which is shorter than for the simulation. Figure 14 shows good quantitative agreement between experiment and simulation, and also identical departure points from the relatively constant settling times observed for lock-in. Both experiment and simulation show a drastic increase in settling time for amplitudes below 5% of the cylinder diameter. These findings suggest good agreement in the dynamics of the flow field, despite the fact that the experiment has a three dimensional flow field compared to the two dimensional nature of the simulation.

Closed loop feedback control

The effect of linear feedback on the global wake flow field for two different phase advances is shown in Figure 15. We compare the experimental results (left portion of the figure) to the CFD simulation reported by Siegel et al.²³ (right portion of Figure 15). At zero phase advance, i.e. pure proportional gain, both experiment and simulation show little effect of the control on the mode amplitudes. While the experiment shows a small increase in amplitudes, the simulation shows a small decrease in mode amplitudes. This may be due to slightly higher gain in the experiment vs. the simulation. At a phase advance of 75 degrees (experiment) / 70 degrees (simulation) the flow shows a transient reduction in mode amplitudes, before the controller loses the ability to stabilize the flow.

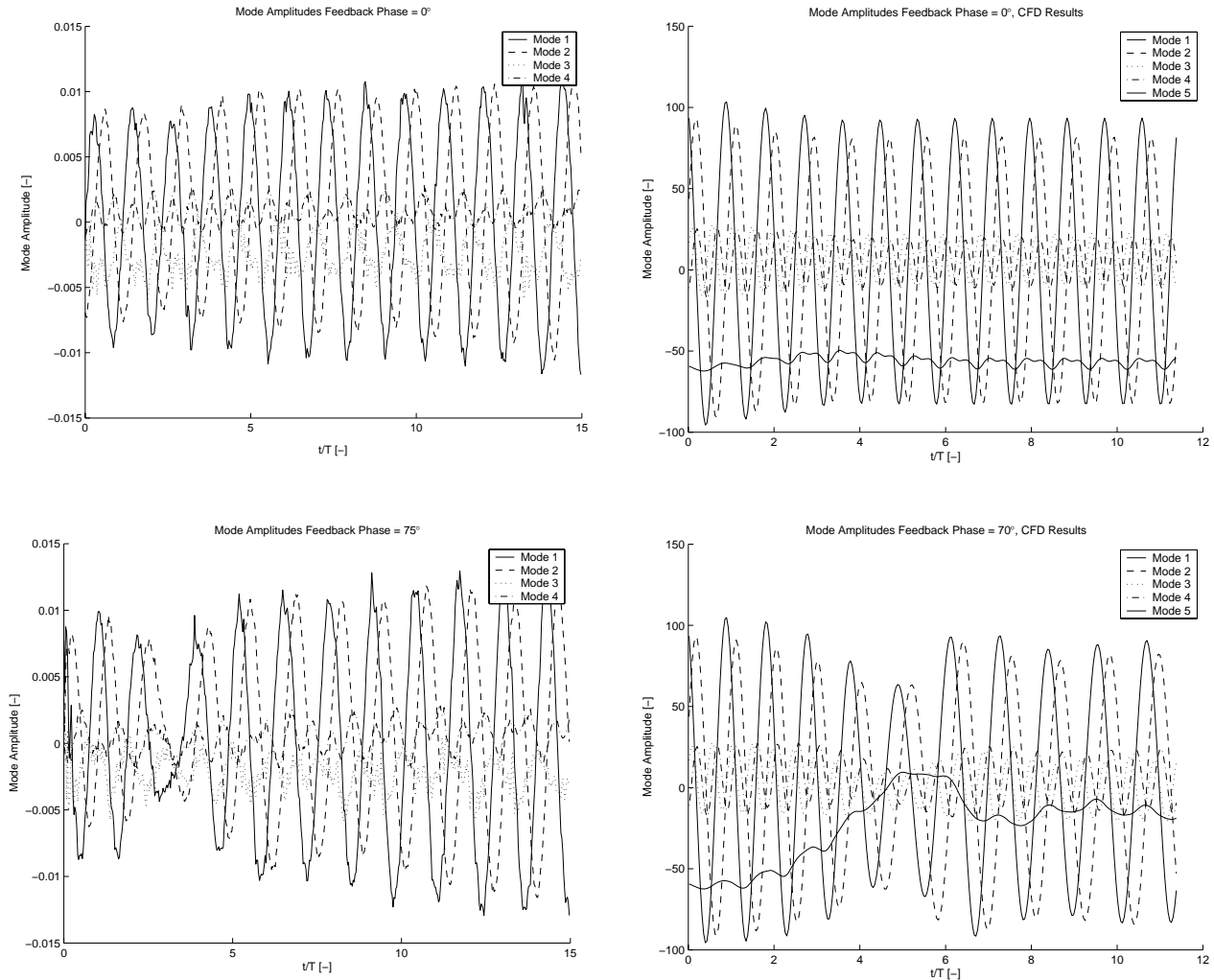


FIGURE 15. Closed loop controlled fixed phase results. Left, water tunnel experiment, right, 2D CFD simulations. Top, Phase advance 0 degree, bottom, phase advance 75 degrees (experiment) / 70 degrees (CFD).

Conclusions

We achieved both qualitative and quantitative agreement between experiment and simulation for transient, open loop forcing. This indicates the ability of the two dimensional simulation to correctly capture the important transient dynamic behavior of the wake flow. Initial closed loop experiments compare favorable with the closed loop simulations conducted using fixed gain feedback. However, difficulties in transient POD mode estimation still exist that need to be overcome in order to be able to repeat the variable gain results obtained in the simulation. While heuristic sensor placement approaches have worked exceedingly well for mode estimation in limit cycle unforced and open loop forced flow fields, transient mode estimation proves to be cumbersome and is still considered deficient.

Outlook

Both low dimensional modeling and mode estimation for transient flow fields remain the challenge for feedback flow control of the cylinder wake. This will be the focus of our research in the near future.

Acknowledgments

The authors would like to acknowledge funding for this research from the Air Force Office of Scientific Research, program monitor Dr. Belinda King and LtCol Sharon Heise. We would also like to acknowledge the fruitful discussions and information exchange with Gilead Tadmor and Bernd Noack. The support of the Dr. Forsythe, Cobalt Solutions, as well as the entire staff of the USAFA Modeling and Simulation Center is greatly appreciated.

References

- 1 Williamson, C.H.K., "Vortex Dynamics in the Cylinder Wake", *Ann. Rev. Fluid Mech.*, 1996, 28:477-539
- 2 Roussopoulos, K., "Feedback control of vortex shedding at low Reynolds numbers", *Journal of Fluid Mechanics*, Vol. 248, 1993, pp. 267-296.
- 3 Park, D. S., Ladd, D. M., and Hendricks, E. W., "Feedback control of von Kármán vortex shedding behind a cylinder at low Reynolds numbers", *Phys. Fluids*, Vol. 6, No.7, 1994, pp. 2390-2405.
- 4 Monkewitz, P. A., "Modeling of self-excited wake oscillations by amplitude equations", *Experimental Thermal and Fluid Science*, Vol. 12, 1996, pp. 175-183.
- 5 Blevins, R., "Flow Induced Vibration", 2nd Edition, Van Nostrand Reinhold, 1990, pp. 54-58.
- 6 Koopmann, G., "The Vortex Wakes of Vibrating Cylinders at Low Reynolds Numbers", *Journal of Fluid Mechanics*, Vol. 28 Part 3, 1967, pp. 501-512.
- 7 Min, C., Choi, H., "Suboptimal Feedback Control of Vortex Shedding at low Reynolds Numbers", *Journal of Fluid Mechanics*, Vol. 401, 1999, pp. 123-156.
- 8 Gillies, E. A., "Low-dimensional characterization and control of non-linear wake flows", PhD. Dissertation, University of Glasgow, Scotland, June 1995.
- 9 Li, F. and Aubry, N., "Reactive flow control for a wake flow based on a reduced model", AIAA Paper 2000-2531, Fluids 2000 Conference and Exhibit, Denver, CO, June 19-22, 2000
- 10 Bewley, T. and Trenchea, C., "Noncooperative Optimization of Controls for Time-Periodic Navier-Stokes Systems (Invited)", AIAA Paper 2002-2754, 3rd Theoretical Fluid Mechanics Meeting, St. Louis, 2002.
- 11 Gillies, E. A., "Low-dimensional control of the cylinder wake", *Journal of Fluid Mechanics*, Vol. 371, 1998, pp. 157-178.
- 12 Cohen, K., Siegel, S., McLaughlin, T., Gillies, E., "Feedback Control of a Cylinder Wake Low Dimensional Model", AIAA Journal, Vol. 41, No.7, 2003.
- 13 Oertel, H. Jr., "Wakes Behind Blunt Bodies", *Annual Review of Fluid Mechanics*, Vol. 22, 1990, pp. 539-564.
- 14 Panton, R.L., "Incompressible Flow", 2nd Edition, John Wiley & Sons, New York, 1996, pp. 384-400.
- 15 Holmes, P., Lumley, J. L., and Berkooz, G., "Turbulence, Coherent Structures, Dynamical Systems and Symmetry", Cambridge University Press, Cambridge, Great Britain, 1996, pp. 86-127.
- 16 Sirovich, L., "Turbulence and the Dynamics of Coherent Structures Part I: Coherent Structures", *Quarterly of Applied Mathematics*, Vol. 45, No. 3, 1987, pp. 561-571.
- 17 Smith, D. R., Siegel, S., and McLaughlin T., "Modeling of the wake Behind a Circular Cylinder Undergoing Rotational Oscillation", AIAA Paper 2002-3066, June 2002.
- 18 Noack, B.R., Afanasiev, K., Morzynski, M. and Thiele, F., "A hierarchy of low-dimensional models for the transient and post-transient cylinder wake", accepted for publication in *J. Fluid Mechanics*, 2003.
- 19 Ahlborn, B., Seto, M., Noack, B., "On drag, strouhal number and vortex street structure", accepted for publication in *J. Fluid Mechanics*, 2003.
- 20 Gerhard, J., Pastoor, M., King, R., Noack, B., Dillman, A., Morzynski, M., Tadmor, G., "Model-based control of vortex shedding using low-dimensional Galerkin models" AIAA Paper 2003-4262, June 2003.
- 21 M. Raffel, C. Willert, J. Kompenhans, "Particle Image Velocimetry", Springer, 1998.
- 22 Siegel, S. Cohen, K., McLaughlin, T., "Real-Time Particle Image Velocimetry for Closed-Loop Flow Control Studies", AIAA 2003-0920, 2003
- 23 Siegel, S. Cohen, K., McLaughlin, T., "Feedback Control of a Circular Cylinder Wake in Experiment and Simulation", AIAA 2003-3569, 2003
- 24 Cohen, K., Siegel, S., McLaughlin, T., "Sensor Placement Based on Proper Orthogonal Decomposition Modeling of a Cylinder Wake", AIAA 2003-4259, 2003